Received: 5 December 2022 | Accepted: 4 July 2023

DOI: 10.1111/jog.15745

ORIGINAL ARTICLE

Identification of N1 methyladenosine-related biomarker predicting overall survival outcomes and experimental verification in ovarian cancer

Jing Zhao[1,2] | Hua Han[2] | Runfang Wang[3] | Yazhuo Wang[2] | Yuan Zhang[2] | Na Li[4] | Bei Wang[2] | Zhaoping Chu[2] | Yunxia Zhang[2] | Hongzhen Zhang[1]

[1]Department of Obstetrics and Gynecology, The First Hospital of Hebei Medical University, Shijiazhuang, China

[2]Department of Gynecology, Hebei General Hospital, Shijiazhuang, China

[3]Department of Obstetrics, Hebei General Hospital, Shijiazhuang, China

[4]Department of Oncology, Hebei General Hospital, Shijiazhuang, China

Correspondence
Hongzhen Zhang, Department of Obstetrics and Gynecology, The First Hospital of Hebei Medical University, 89 Dong Gang Road, Shijiazhuang, Hebei Province 050000, China.
Email: hbmu_zhanghongzhen@163.com

Funding information
the Scientific Research Foundation of the Hebei Health Commission, Grant/Award Numbers: 20200754, 20220862

Abstract

Aim: This study aimed to construct a N1-methyladenosine (m1A)-related biomarker model for predicting the prognosis of ovarian cancer (OVCA).

Methods: OVCA samples were clustered into two subtypes using the Non-Negative Matrix Factorization (NMF) algorithm, including TCGA ($n = 374$) as the training set and GSE26712 ($n = 185$) as the external validation set. Hub genes, which were screened to construct a risk model, and nomogram to predict the overall survival of OVCA were explored and validated through various bioinformatic analysis and quantitative real-time PCR.

Results: Following bootstrap correction, the C-index of nomogram was 0.62515, showing reliable performance. The functions of DEGs in the high- and low-risk groups were mainly enriched in immune response, immune regulation, and immune-related diseases. The immune cells relevant to the expression of hub genes were explored, for example, Natural Killer (NK) cells, T cells, activated dendritic cells (aDC).

Conclusions: *AADAC*, *CD38*, *CACNA1C*, and *ATP1A3* might be used as m1A-related biomarkers for OVCA, and the nomogram labeled with m1A for the first time had excellent performance for predicting overall survival in OVCA.

KEYWORDS
immune infiltration, N1-methyladenosine, nomogram, ovarian cancer, prognosis

INTRODUCTION

Ovarian cancer (OVCA) is the malignant tumor that poses the greatest threat to women's health, ranking third in incidence and first in mortality in the female reproductive system.[1] There were nearly 239 000 new OVCA cases and 152 000 new OVCA deaths each year worldwide, accounting for 3.6% of all new cancer cases and 4.3% of all cancer deaths.[2] Due to the lack of effective screening strategies and a few early-stage clinical symptoms, about 60% of patients with epithelial OVCA are underdiagnosed and too late.[3] Despite the widespread use of surgery, chemotherapy, biological therapy, and targeted gene therapy in the treatment of OVCA,[4] the 5-year survival rate for OVCA is still only 35%–38%.[5] Exploring the alternative pathogenesis of OVCA is of great significance for early detection, early diagnosis, and early treatment.[6,7]

As a vital RNA methylation modification, N1-methyladenosine (m1A) is ubiquitous in tRNA, rRNA, mRNA, and mitochondrial transcripts, and m1A dysregulation affected various cellular processes.[8,9] The latest study found that m1A methylation modification plays a crucial role in the prognosis and the shaping of the immune microenvironment of OVCA.[10] Another report in the literature suggested that the m1A-regulating enzyme TRMT10C affected the survival of OVCA patients.[11] In the other words, the underlying significances of m1A dysregulation in the progression of OVCA have been preliminarily inspired, while, no theory has conducted a theoretical system exploring the targeted binding sites as well as the regulatory networks of m1A-related genes affecting OVCA.

Li et al. used weighted gene co-expression network analysis (WGCNA) and nonnegative matrix factorization (NMF) method sample classification to identify key

biomarkers in CD8 T cell-related genes and construct prognostic features in OVCA.[12] Chen et al. explored the underlying mechanisms of the tumorigenesis and progression based on genes associated with OVCA clinical features.[13] Considering the advantages of bioinformatics analysis recognizing markers in various tumors, in this study, according to the previous literature,[8,14,15] 10 m1A genes were collected to cluster OVCA patients into two tumor subtypes to excavate pivotal m1A-related biomarkers. Therefore, a four genes-based m1A-related OVCA risk model and nomogram were constructed and evaluated for the first time, providing a reference for diagnosing and treatment of OVCA cohorts. And meanwhile, correlation analysis of hub genes expression and key immune cells was helpful to reveal the underlying roles of immune-related therapy targeting hub genes in OVCA progression. The workflow chart of this study is shown in Supporting Information Figure S1.

MATERIALS AND METHODS

Data collection

We downloaded OVCA-related expression data from The Cancer Genome Atlas (TCGA, https://portal.gdc.cancer.gov/) database and Gene Expression Omnibus (GEO, https://www.ncbi.nlm.nih.gov/geo/) database. m1A genes were retrieved from published literature[8,14,15] including *TRMT10C*, *TRMT61B*, *TRMT6*, *TRMT61A*, *ALKBH3*, *ALKBH1*, *YTHDC1*, *YTHDF1*, *YTHDF2*, and *YTHDF3*. A total of 379 samples were included in the TCGA database, 5 recurrence samples were removed, and 374 samples with clinical information were used for subsequent analysis. A total of 185 OV patients with survival information were included in the GSE26712 dataset.

Non-negative matrix factorization clustering

Based on the expressed profiles of 10 m1A genes, NMF clustering analysis were first performed using the NMF (version 0.23.0) R package[16] to cluster the TCGA-OVCA samples into different subtypes. Survival analysis was then performed for the different subtypes using the survminer (version 0.4.9) R package.[17] The clinicopathological factors such as age, stage, race, chemotherapy, and radiotherapy were added to compare whether there was a difference between samples of different subtypes by chi-square test and $p < 0.05$ was considered as a significant difference.[18]

Differentially expressed genes screening

We used the DESeq2 R package (version 1.34.0, https://bioconductor.org/packages/release/bioc/html/DESeq2.html) to compare the differences in mRNA expression levels of different subtypes. The screening conditions for the DEGs were $|\log2FC| > 0.5$, adj.$p < 0.05$.

Screening for hub genes

We used the TCGA-OVCA samples ($n = 373$) as the training set of the model to construct a least absolute shrinkage and selection operator (LASSO) regression model using the DEGs between the two subtypes. To reduce the feature dimension, we used the glmnet R package[19] (version 4.1-3), set the parameter famil to cox, implemented lasso logistic regression, and used 10-fold cross-validation to calculate the error rate under different features to select strongly correlated features.

Genes screened by lasso regression were subjected to univariate COX regression analysis. Those with $p < 0.01$ were subjected to multivariate cox regression analysis to screen hub genes and used to construct a risk model.

Construction and validation of the risk model

The risk score was calculated using the predict.coxph function scores through survival (version 3.2-13) R package,[17] where the risk score of each patient in TCGA-OVCA was calculated as follows: $\text{Risk score} = \text{EXP}_{AADAC} \times (-0.095) + \text{EXP}_{CD38} \times (-0.15) + \text{EXP}_{CACNA1C} \times 0.15 + \text{EXP}_{ATP1A3} \times 0.11$. That is, a risk model was constructed based on the predictive genes and coefficients obtained by COX regression analysis. K–M survival curve between the high and low-risk groups were conducted as well. To further assess the validity of the risk model, the survival ROC (version 1.03) R package (https://CRAN.R-project.org/package=survivalROC) was used to draw the ROC curve with 3-, 5-, and 7- years as survival time nodes. Validation of the applicability was made in GSE26712.

After univariate and multivariate COX regression analyses, we constructed a nomogram of 3-, 5-, and 7-year survival rates for the prognosis of OVCA. Calibration curve was drawn after that. The closer the slope was to 1, the more accurate the prediction was. We further performed a decision curve analysis (DCA) to validate this model's diagnostic accuracy and clinical utility.

Enrichment analysis of the DEGs between high- and the low-risk groups

We first used the DESeq2 R package (version 1.34.0) to obtain the DEGs between high- and low-risk samples. The filter conditions were $|\log2FC| > 1$ and adj.$p < 0.05$. Afterward, the clusterProfiler R language[20] (version 4.2.1) was used to perform Gene Ontology (GO) and Kyoto Encyclopedia of Genes and Genome (KEGG) enrichment analysis on DEGs, and the GO

plot (version 1.0.2) and enrich plot packages (version 1.10.2, https://github.com/huerqiang/enrichplot) were utilized to draw GO enrichment graph and bubble graphs. In addition, we also performed GSEA enrichment analysis on the prognosis-related genes that were finally determined to build the risk model to find the functions and related pathways between high and low-risk groups. The significance threshold of single-gene GSEA was $|NES| > 1$, p-val<0.05, and q-val<0.2 as screening conditions.

The ceRNA regulatory network and immune correlation analysis relevant to hub genes

In order to investigate the potential regulatory mechanism targeting the hub genes, the starbase database (https://starbase.sysu.edu.cn/) was used to predict potential binding sites of hub genes for establishment of the lncRNA–miRNA–mRNA networks, where miRNA is the core regulatory factor, that is, lncRNAs that competitively bound to miRNAs could regulate the transcription level of mRNA that was regulated by corresponding miRNAs. Hence, the opposite expression patterns between miRNAs and hub genes (screening criteria: CLIP-DATA ≥ 1) as well as the interaction of lncRNAs and miRNAs involved (screening criteria: CLIP-DATA ≥ 5) were included to reduce false-positive rate and exhibited through the Cytoscape[21] (version 3.8.2) software.

Besides, immune cell correlation analysis was performed using the GSVA (version 1.34.0) R package to interpret gene expression data by ssGSEA.[22] Correlations were evaluated through Spearman tests. The statistical difference was considered to be significant at $p < 0.05$.

Exploration of hub gene expression

After obtaining the patient's informed consent and approval from the Ethics Committee of Hebei General Hospital, the tissues we collected were immediately stored at −80°C until use. We extracted total RNA from 15 ovarian cancer tissues and 15 normal tissue samples using TRizol reagent (Thermo Fisher Scientific, Waltham, MA). Afterward, cDNA was obtained using a FastQuant First Strand cDNA Synthesis kit (TIANGEN, Beijing, China). qPCR was conducted using the SYBR Green PCR kit (TIANGEN, Beijing, China) according to the protocol. The primer sequences pairs of hub genes used in this study were designed as follows: *AADAC*-F (5′-TGCAGGAGGGAATTTAGCTG-3′)/*AADAC*-R (5′-TGACATCTGGGTCATCAAGG-3′); CD38-F (5′-ACAGACCTGGCTG

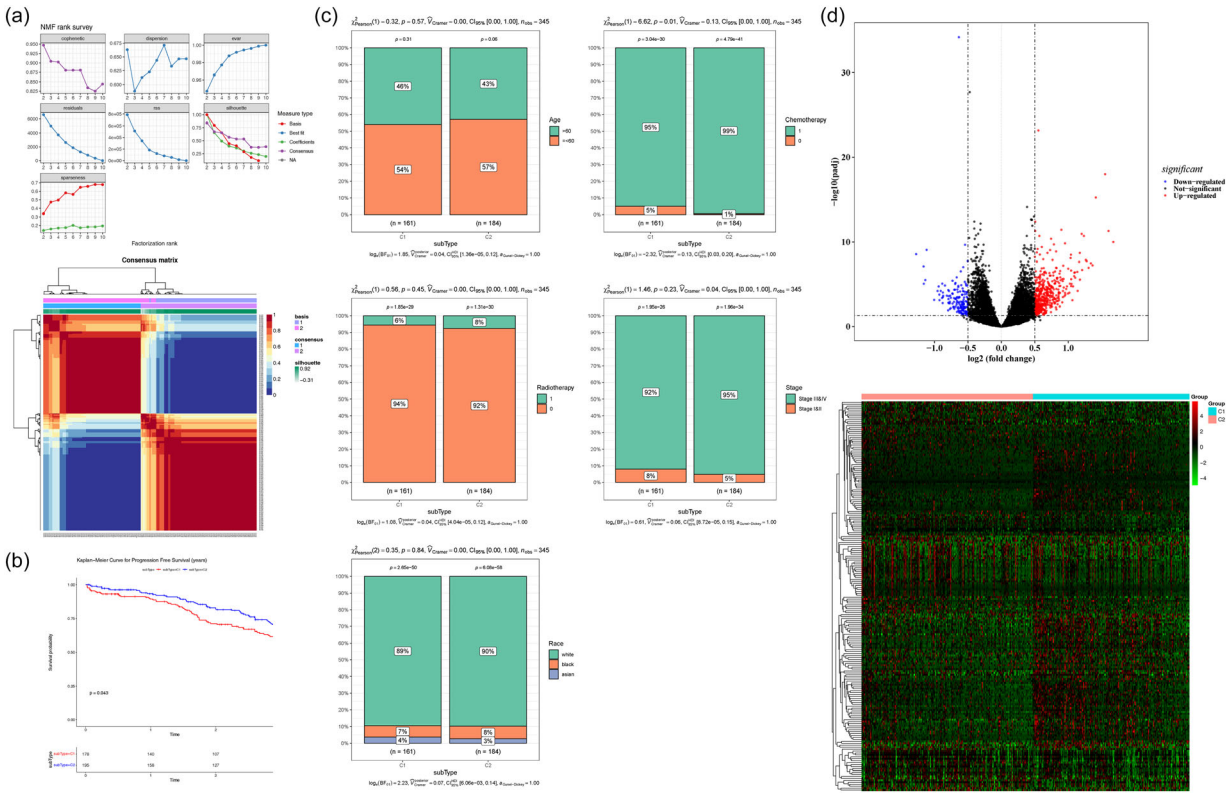

FIGURE 1 Identification of the molecular subtypes of TCGA-OVCA cohorts using NMF cluster analysis. (a) The cophenetic, dispersion, evar, residuals, rss, silhouette, and sparseness distributions when rank k was set as 2–10, in which $k = 2$ was considered as the optimal cluster number, and consensus map of NMF clustering for $k = 2$ was displayed. (b) Kaplan–Meier (K–M) survival analysis in C1 and C2 groups ($p = 0.043$). (c) Clinical correlation analysis of C1 and C2 groups with different clinicopathological factors (chi-square test). (d) The volcano plot and heatmap of differentially expressed genes (DEGs) between two subtypes of TCGA-OVCA cohort.

CCGCCTCTCTAG-3′)/*CD38*-R (5′-GGGGCGTAGTC-TTCTCTTGTGATGT-3′); *CACNA1C*-F (5′-GAAGC-GGCAGCAATATGGGA-3′)/*CACNA1C*-R (5′-TTGG TGGCGTTGGAATCATCT-3′); *ATP1A3*-F (5′-GCAA-CGAGACTGTGGAGGACAT-3′)/*ATP1A3*-R (5′-GAC-TTCCTGTAACAACGCATC-3′); *β-actin*-F (5′-ATG ACTTAGTTGCGTTACACC-3′)/*β-actin*-R (5′-GACTT-CCTGTAACAACGCATC-3′), using *β-actin* as house-keeping gene. All data were calculated using the $2 - \Delta\Delta Ct$ method.

RESULTS

Two m1A subtypes were identified based on 10 m1A genes expressions

After excluding one sample without survival data, NMF clustering was conducted to cluster the 374 samples in TCGA-OVCA into two m1A subtypes through the NMF algorithm (k = 2, C1 = 179, C2 = 195, see Figure 1a). Survival results showed there were significant differences in individuals' prognosis between two subtypes, and cohorts within C2 groups had greater survival probability ($p = 0.043$) (Figure 1b). The results for gene expression of 10 m1A genes exhibited that the up-regulation of these m1A genes might be relevant to poorer prognosis of OVCA patients (Supporting Information Figure S2). In addition, substantial differences in chemotherapy were found between different subtype clusters in two m1A subtypes ($p = 0.01$), while there was no distinct difference in other clinical subtype clusters (Figure 1c).

Four prognostic related hub genes were identified to construct the risk model

The 609 DEGs (455 up-regulated and 154 down-regulated gene) between the two m1A expression subtypes were included to construct a lasso regression

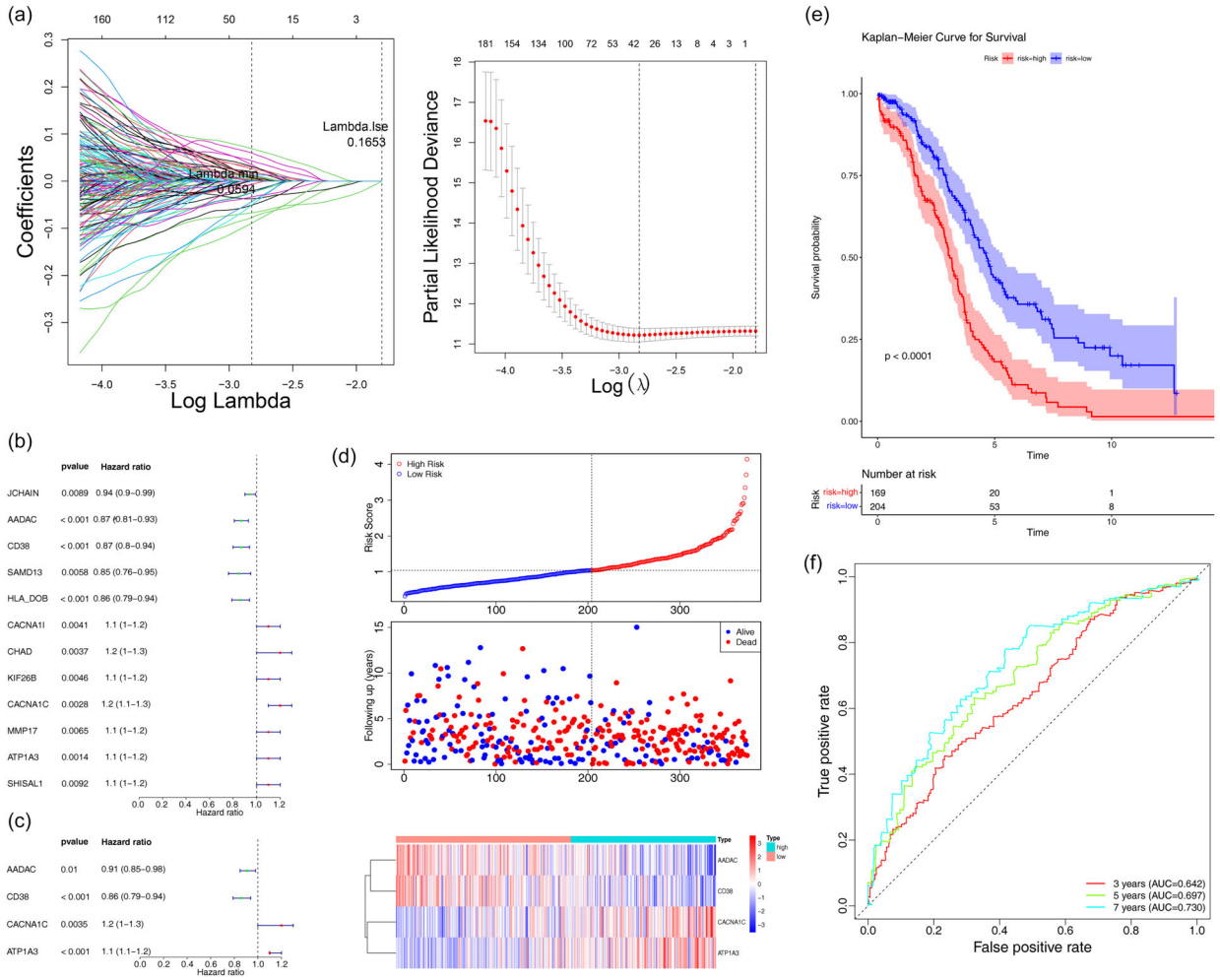

FIGURE 2 Construction and evaluation of a predictive model for TCGA-OVCA. (a) LASSO regression analysis to select prognostic genes, including (left) lasso penalty coefficient plot and (right) lasso cross-validation error plot. (b,c) Univariate and multivariate COX analysis forest plot. (d) Distribution of risk curve, survival state and genes expression of individuals in TCGA-OVCA. (e) K–M survival curve between high- and low- risk groups ($p < 0.0001$). (f) Receiver operating characteristic (ROC) curve for survival prediction at 3-, 5-, and 7-years.

prognostic model (Figure 1d) and 37 prognostic-related genes were screened ($\lambda = 0.0594$; Figure 2a). Moreover, *AADAC*, *CD38*, *CACNA1C*, and *ATP1A3* were finally identified as hub genes for constructing the risk model (Figure 2b,c). Then OVCA patients were divided into high and low-risk groups according to the best cut-off (1.039795) value of the risk score, with 169 samples in the high-risk group and 204 in the low-risk group. Representatives from the high-risk group had higher risk scores and a higher risk of death than the low-risk group. And meanwhile, the expression of *AADAC* and *CD38* was higher in the low-risk group, whereas *CACNA1C* and *ATP1A3* were higher in the high-risk group (Figure 2d). This result is consistent with the multivariate regression analysis. The survival curve indicated that the survival rate of patients in the high-risk group was lower than that in the low-risk cohort ($p < 0.0001$) (Figure 2e). It was observed that AUCs at 3-, 5-, and 7- years were all greater than 0.6, indicating that the performance of the risk model is better (Figure 2f). Moreover, the survival distributions (Figure 3a), survival probability (Figure 3b), as well as ROC curve (Figure 3c) for the risk model were validated in GSE26712, in which the survival difference between different risk groups was observed ($p < 0.013$). And the AUC values were similar to the previous results (AUC > 0.6). These findings further confirmed the predictive value and stability of the model.

Clinical correlation analysis and nomogram establishment

Clinical correlation analysis through Wilcoxon test showed that there were distinct differences in the risk score between the two m1A subtypes (C1 and C2) as well as individuals with different stage and chemotherapy terms (Figure 4a). In comparison, only subtype was quite different between high- and low-risk groups ($p < 0.001$, chi-square test; Table 1). Similarly, the heat map for hub genes expression in different clinical subtypes showed that *AADAC* and *CD38* were highly expressed in the low-risk group and C2, while *CACNA1C* and *ATP1A3*

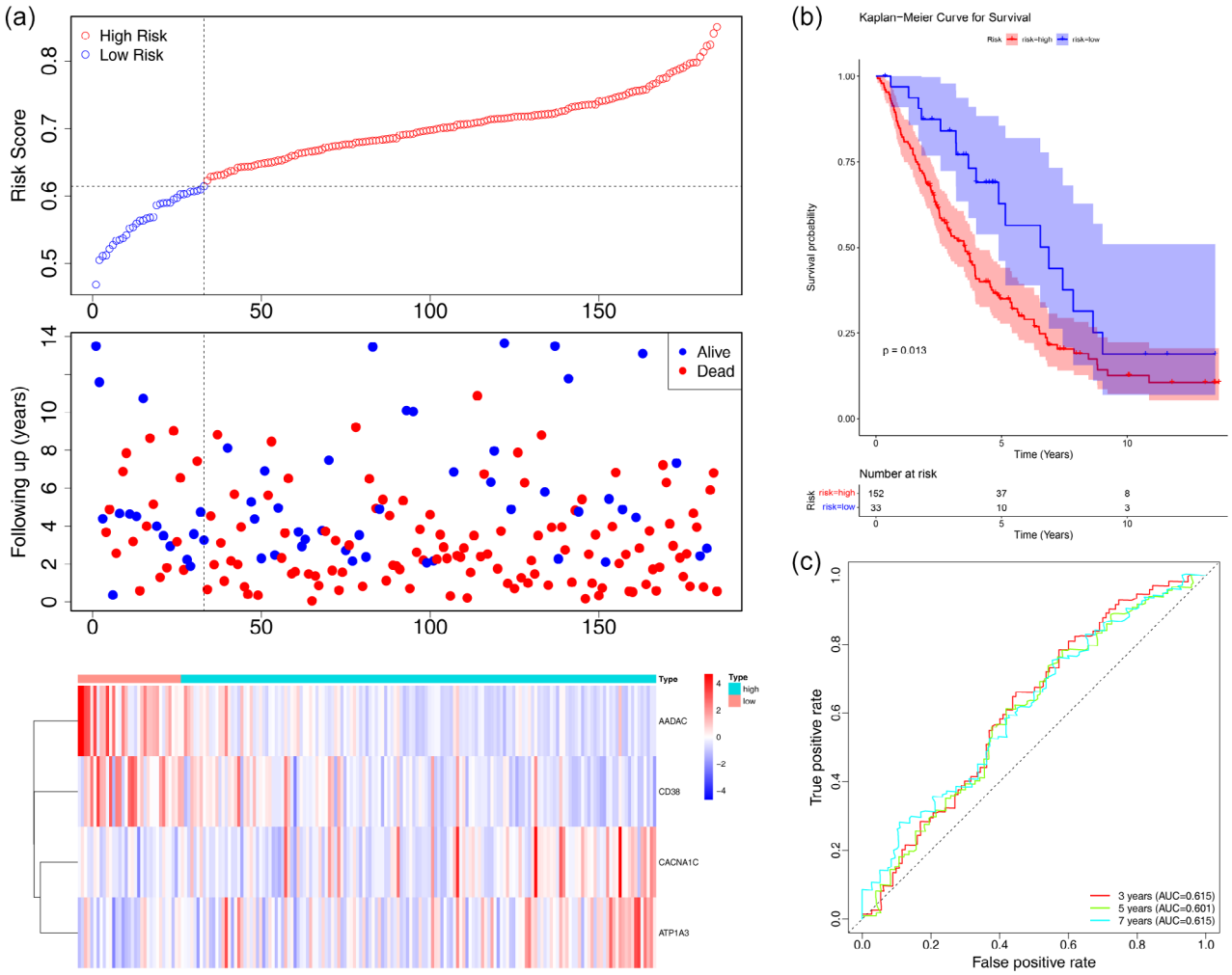

FIGURE 3 Validation of the predictive model in GSE26712. (a) Distribution of risk curve, survival state, and genes expression of individuals in GSE26712. (b) K–M survival curve between high- and low- risk groups ($p = 0.013$). (c) ROC curve for survival prediction at 3-, 5-, and 7-years.

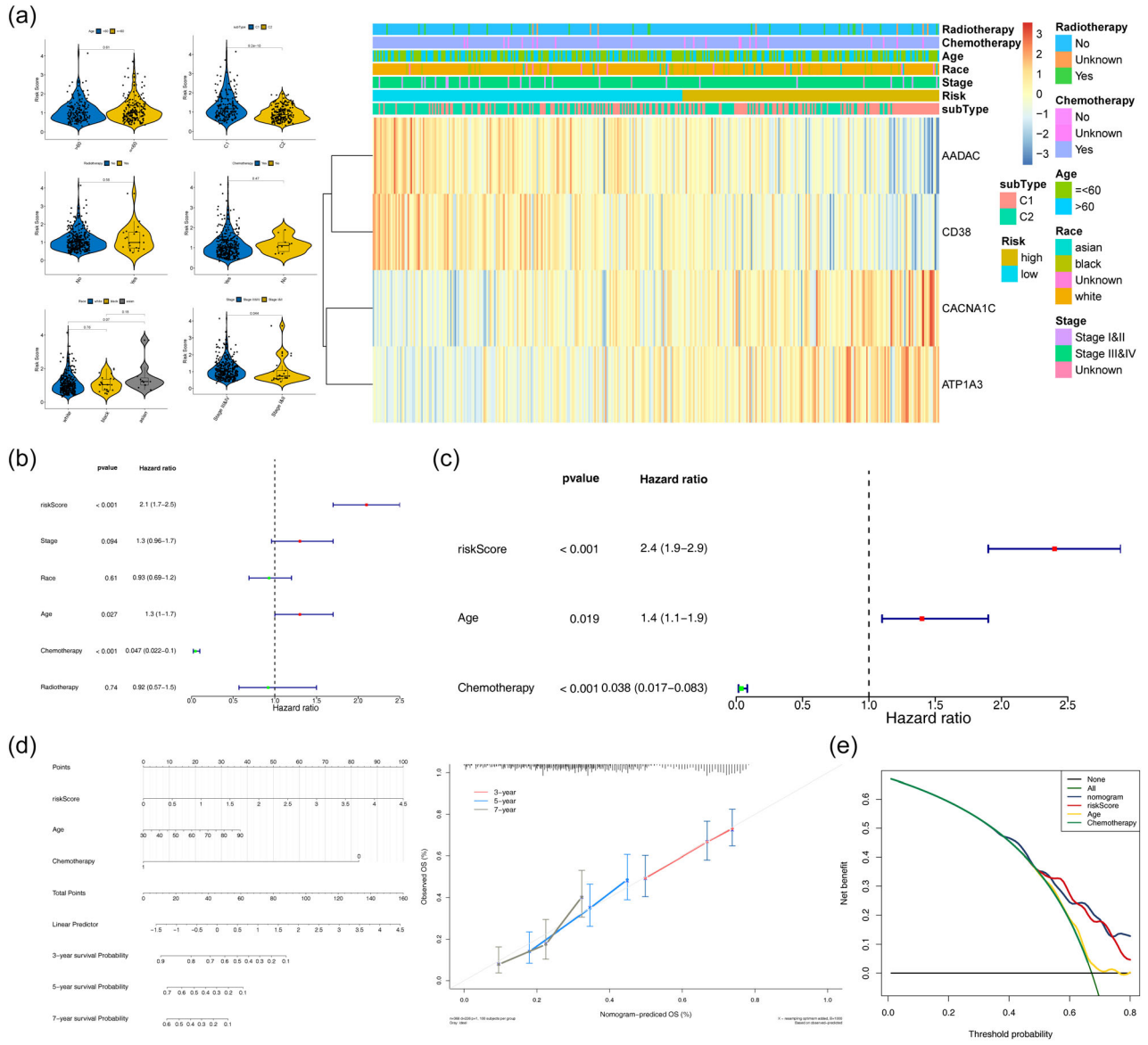

FIGURE 4 Independent prognostic analysis and construction of a nomogram model. (a) Violin plots and heat map for correlation between risk score and various clinical characteristics. (b,c) Univariate and multivariate COX analysis forest plot. (d) The nomogram of the risk model based on the risk score and other independent prognostic factors, and corresponding calibration curve. (e) Decision curve analysis (DCA) to evaluate the clinical utilize of the nomogram.

were highly expressed in the high-risk group and C1, remaining consistent with previous results.

The univariate and multivariate COX regression analyses including risk score and clinicopathological factors showed that the three elements of chemotherapy, age, and risk score were statistically different ($p < 0.05$; Figure 4b,c). Hence, the nomogram based on the risk model as well as chemotherapy, age was constructed. The c-index of which was 0.62499, and the adjusted c-index was 0.62515 (Figure 4d), indicating that the predictive strength of the model was reliable. DCA curve showed that the benefits of risk score and multivariate models were higher than extreme curves, suggesting that they have a larger optional range and are relatively safe (Figure 4e).

Enrichment analysis on DEGs between high and low-risk groups

Difference analysis showed that there were 140 DEGs between high and low-risk groups, of which 44 mRNAs were up-regulated in the high-risk group, and 96 mRNAs were down-regulated in the high-risk group (Figure 5a). The GO/KEGG enrichment analyses on the DEGs further revealed that these genes were mainly related to the activation of chondrocyte differentiation, as well as the inhibition of the granulocyte chemotaxis process (Figure 5b), and so on. In the meantime, the pathways of primarily in the interaction of viral proteins with cytokine–cytokine receptor interaction were enriched in

TABLE 1 Correlation analysis between risk score and clinical characteristics through chi-square test.

		Score		
	Total ($N = 373$)	**High ($N = 169$)**	**Low ($N = 204$)**	***p*-value**
Age				0.988
≤60	204 (54.7%)	93 (55.0%)	111 (54.4%)	
>60	169 (45.3%)	76 (45.0%)	93 (45.6%)	
Stage				0.194
Stages I and II	22 (5.9%)	6 (3.6%)	16 (7.8%)	
Stages III and IV	348 (93.3%)	162 (95.9%)	186 (91.2%)	
Unknown	3 (0.8%)	1 (0.6%)	2 (1.0%)	
Race				0.515
Asian	11 (2.9%)	7 (4.1%)	4 (2.0%)	
Black	25 (6.7%)	13 (7.7%)	12 (5.9%)	
Unknown	13 (3.5%)	5 (3.0%)	8 (3.9%)	
White	324 (86.9%)	144 (85.2%)	180 (88.2%)	
Chemotherapy				0.276
No	10 (2.7%)	7 (4.1%)	3 (1.5%)	
Unknown	12 (3.2%)	5 (3.0%)	7 (3.4%)	
Yes	351 (94.1%)	157 (92.9%)	194 (95.1%)	
Radiotherapy				0.792
No	341 (91.4%)	153 (90.5%)	188 (92.2%)	
Unknown	9 (2.4%)	5 (3.0%)	4 (2.0%)	
Yes	23 (6.2%)	11 (6.5%)	12 (5.9%)	
subType				<0.001
C1	178 (47.7%)	100 (59.2%)	78 (38.2%)	
C2	195 (52.3%)	69 (40.8%)	126 (61.8%)	

KEGG (Figure 5c), and so on. To avoid the omission of some genes whose differential expression was not significant but biologically significant, we also performed a GSEA enrichment analysis, where adaptive immune response, T cell activation, as well as graft-versus-host disease were found (Figure 5e).

Construction of ceRNA network and immune correlation analysis

To further explore the upstream regulatory mechanisms of hub genes, a total of 31 miRNAs target to hub genes as well as 38 lncRNAs binding sites of these miRNAs were determined and conducted to construct the miRNA–mRNA regulatory network (Figure 6a), in which *CACNA1C* was predicted as only the binding sites of hsa-miR-384, and it was competitively bound by among *lncRNAs SNHG8, NEAT1, MALAT1, AC005261.1*, and *NORAD. AADAC* and *CD38* were targeted by many miRNAs and lncRNAs in the network, suggesting that ceRNAs may be important in regulating the expressions of which.

Moreover, the expression levels of *AADAC* were significantly positively correlated with activated dendritic cells (aDC), dendritic cells (DC), macrophages, neutrophils, T cells, T helper cells, T-helper 1 (Th1) cells, and regulatory T cells (Tregs). However, the expression levels of *AADAC* were significantly negatively correlated with Natural Killer (NK) cells. The expression level of *ATP1A3* was positively correlated with B cells, cytotoxic cells, neutrophils, central memory T cells (Tcm), effector memory T cells (Tem), follicular helper T cells (Tfh), Th1 cells, and Treg. The expression level of *CACNA1C* was negatively correlated with aDC, T-helper type 17 (Th17) cells but positively correlated with CD8 T cells, NK CD56dim cells, T helper cells, and T-helper type 2 (Th2) cells. The expression level of CD38 was positively correlated with Mast cells, T gamma delta (Tgd), and Th17 cells (Figure 6b).

Exploration of prognostic gene expression

Using the RT-qPCR methods, it was found that the expressions of *AADAC*, *ATP1A3*, and *CD38* were higher

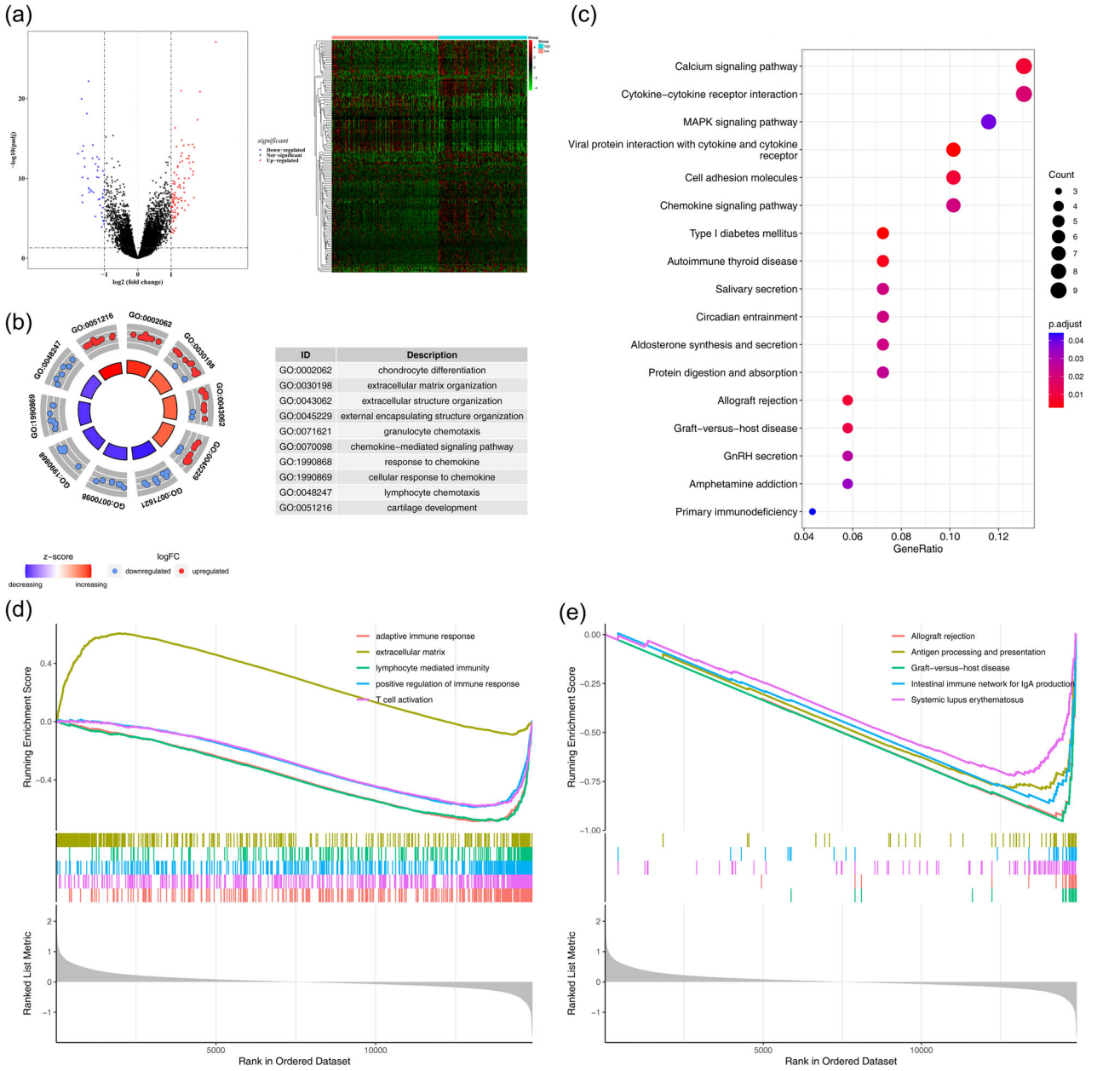

FIGURE 5 Functional enrichment analysis of DEGs between high and low-risk groups. (a) Volcano plot and heatmap of DEGs between high and low-risk groups. (b) The circle map of Gene Ontology (GO) enrichment analysis. (c) The bubble plot of Kyoto Encyclopedia of Genes and Genome (KEGG) enrichment analysis. (d,e) The enriched GO and KEGG terms by Gene Set Enrichment Analysis (GSEA).

in ovarian cancer tissues but lower in normal tissues. *CACNA1C* was more deficient in cancer tissues and higher in normal, and all the differences were statistically significant (Figure 6c), which were consistent with the expression in TCGA.

DISCUSSION

Previous studies showed that m1A regulatory molecules can affect the processes of transcription and translation to promote tumorigenesis.[23,24] The latest research demonstrated that m1A methylation modification is an essential driver in the prognosis of OVCA.[10] Considering the potential prognostic value of various RNA methylation modifications in OVCA,[25–27] we used the NMF algorithm for the first time to cluster OVCA samples and screened out four hub genes (*AADAC*, *CD38*, *CACNA1C*, and *ATP1A3*) for building a risk score model in this study.

AADAC is a glycoprotein and is associated with lower rifapentine clearance.[28] A synergistic tumor suppressor effect between *AADAC* and anticancer drugs was also found, suggesting that *AADAC* is beneficial to the prognosis of OVCA patients, which is consistent with our

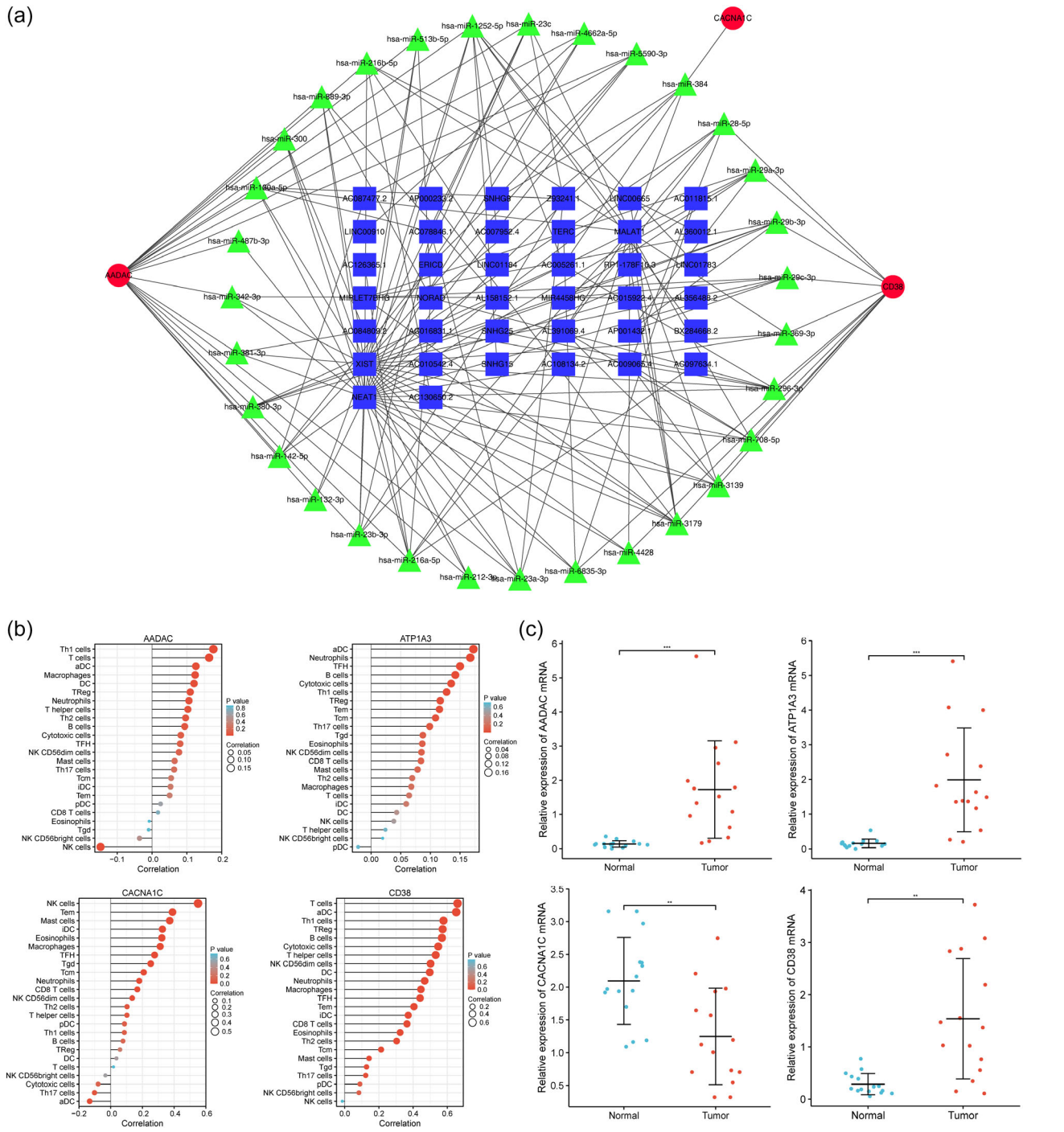

FIGURE 6 Exploration of hub genes. (a) The ceRNA network targeting to hub genes. Red circle represents hub gene, green triangle represents miRNA, and blue square represents lncRNA. (b) Immune infiltration analysis of hub genes, including activated dendritic cells (aDC), dendritic cells (DC), macrophages, neutrophils, T cells, T helper cells, T-helper 1 (Th1) cells, regulatory T cells (Tregs), natural killer (NK) cells, B cells, cytotoxic cells, central memory T cells (Tcm), effector memory T cells (Tem), follicular helper T cells (Tfh), T-helper type 17 (Th17) cells, CD8 T cells, NK CD56dim cells, NK CD56bright cells, T-helper type 2 (Th2) cells, Mast cells, plasmacytoid dendritic cells (pDC), immature dendritic Cells (iDC), Eosinophils, T gamma delta (Tgd). (c) The expressions of four hub genes in OVCA and normal tissues.

experimental results.[29] *CD38* is widely expressed in various human tissues and cells and plays an important role in the immune system. The great success of *CD38*-targeted antibodies in treating multiple myeloma has driven its research in other oncology areas.[30] Zhu et al. demonstrated that *CD38* predicts a favorable prognosis by enhancing immune invasion and anti-tumor immunity in the OVCA microenvironment.[31] There is evidence that *CACNA1C* plays a crucial role in regulating the occurrence and development of various tumors by targeting

the immunity of patients, which may be a novel prognostic marker for OVCA.[32] As a member of the *ATP1A* gene family, *ATP1A3* can promote tumor proliferation, invasion, anti-apoptosis, and cell cycle arrest.[33] The latest study found that high expression of *ATP1A3* is associated with poor prognosis in ovarian cancer patients.[34] Our study verified the expressions of four hub genes in OVCA and normal tissues. The expressions of *AADAC*, *ATP1A3*, and *CD38* in OVCA were higher than that in normal, while *CACNA1C* was contrary, which was consistent with the current research results. Immune correlation analysis showed that the expression of hub genes was correlated with immune cell infiltration, suggesting that all the four genes could influence tumor progression. Our results were consistent with the current research.

Cramer and Welch proposed in 1983 that excessive gonadotropin stimulation can lead to ovarian cancer.[35] Many studies have shown that GnRH and its synthetic analogs have direct anti-proliferative effects on OVCA cell lines.[36] The analysis in this study enriched the gonadotropin-releasing hormone secretion pathway, suggesting that the risk model may be related to the sex hormone secretion status of OVCA patients. For the lncRNA–miRNA–mRNA ceRNA network of these four genes, it was found that long non-coding RNAs *XIST* and *NEAT1* formed the most connections with miRNA-mRNAs. The latest study found that inhibition of *XIST* upregulates microRNA-149-3p to repress ovarian cancer cell progression.[37] Yang et al. showed that *NEAT1* promotes the proliferation of ovarian cancer cells and angiogenesis of co-incubated human umbilical vein endothelial cells by regulating *FGF9* through sponging miR-365.[38] Our study provided a theoretical basis for further exploration of their mechanism of action, while the current research is limited to bioinformatics analysis and simple expression verification.

Above all, this study was employed to make a cluster analysis of OVCA samples to construct a nomogram with m1A as a tag for the first time, where the expression of four m1A-related biomarkers was converted into a score to take all of which into consideration for clinical utilize. Simultaneously, the mRNA expression of these four hub genes was confirmed using clinical samples and was considered reliable potential detection targets. Besides, the immune cell targets and ceRNA network associated with hub genes were excavated, laying the foundation for further exploring the impact and underlying mechanism of m1A on OVCA.

ACKNOWLEDGMENTS

This study was funded by the Scientific Research Foundation of the Hebei Health Commission (No. 20200754 and No. 20220862).

CONFLICT OF INTEREST STATEMENT

The authors declare no conflicts of interest.

DATA AVAILABILITY STATEMENT

The data that support the findings of this study are openly available at: doi:10.6084/m9.figshare.22332289.

ORCID

Jing Zhao https://orcid.org/0000-0002-1557-9022
Yazhuo Wang https://orcid.org/0000-0003-3952-9553
Na Li https://orcid.org/0000-0003-0178-4743

REFERENCES

1. Siegel RL, Miller KD, Jemal A. Cancer statistics, 2020. CA Cancer J Clin. 2020;70(1):7–30.
2. Lheureux S, Braunstein M, Oza AM. Epithelial ovarian cancer: evolution of management in the era of precision medicine. CA Cancer J Clin. 2019;69(4):280–304.
3. Berek JS, Renz M, Kehoe S, Kumar L, Friedlander M. Cancer of the ovary, fallopian tube, and peritoneum: 2021 update. Int J Gynaecol Obstet. 2021;155 Suppl 1(Suppl 1):61–85.
4. Feng Z, Wen H, Bi R, Yang W, Wu X. Prognostic impact of the time interval from primary surgery to intravenous chemotherapy in high grade serous ovarian cancer. Gynecol Oncol. 2016;141(3):466–70.
5. Siegel RL, Miller KD, Jemal A. Cancer statistics, 2016. CA Cancer J Clin. 2016;66(1):7–30.
6. Salani R, Backes FJ, Fung MF, Holschneider CH, Parker LP, Bristow RE, et al. Posttreatment surveillance and diagnosis of recurrence in women with gynecologic malignancies: Society of Gynecologic Oncologists recommendations. Am J Obstet Gynecol. 2011;204(6):466–78.
7. Wu DD, Chen X, Sun KX, Wang LL, Chen S, Zhao Y. Role of the lncRNA ABHD11-AS(1) in the tumorigenesis and progression of epithelial ovarian cancer through targeted regulation of RhoC. Mol Cancer. 2017;16(1):138.
8. Chi Z, Jia G. Reversible RNA modification N1-methyladenosine (m1A) in mRNA and tRNA. Genomics Proteomics Bioinformatics. 2018;16(3):7.
9. Dominissini D, Nachtergaele S, Moshitch-Moshkovitz S, Peer E, Kol N, Ben-Haim MS, et al. The dynamic N(1)-methyladenosine methylome in eukaryotic messenger RNA. Nature. 2016;530(7591):441–6.
10. Liu J, Chen C, Wang Y, Qian C, Wei J, Xing Y, et al. Comprehensive of N1-Methyladenosine modifications patterns and immunological characteristics in ovarian cancer. Front Immunol. 2021;12:746647.
11. Wang Q, Zhang Q, Huang Y, Zhang J. M(1)a regulator TRMT10C predicts poorer survival and contributes to malignant behavior in gynecological cancers. DNA Cell Biol. 2020;39(10):1767–78.
12. Li L, Chen D, Luo X, Wang Z, Yu H, Gao W, et al. Identification of CD8(+) T cell related biomarkers in ovarian cancer. Front Genet. 2022;13:860161.
13. Chen J, Cai Y, Xu R, Pan J, Zhou J, Mei J. Identification of four hub genes as promising biomarkers to evaluate the prognosis of ovarian cancer in silico. Cancer Cell Int. 2020;20:270.
14. Safra M, Sas-Chen A, Nir R, Winkler R, Nachshon A, Bar-Yaacov D, et al. The m1A landscape on cytosolic and mitochondrial mRNA at single-base resolution. Nature. 2017;551(7679):251–5.
15. Anreiter I, Mir Q, Simpson JT, Janga SC, Soller M. New twists in detecting mRNA modification dynamics. Trends Biotechnol. 2021;39(1):72–89.
16. Gaujoux R, Seoighe C. A flexible R package for nonnegative matrix factorization. BMC Bioinformatics. 2010;11:367.
17. Lin H, Zelterman D. Modeling survival data: extending the cox model. Dent Tech. 2022;44:85–6.

18. Patil I. Visualizations with statistical details: the 'ggstatsplot' approach. J Open Source Softw. 2021;6(61):3167.
19. Friedman J, Hastie T, Tibshirani R. Regularization paths for generalized linear models via coordinate descent. J Stat Softw. 2010; 33(1):1–22.
20. Yu G, Wang LG, Han Y, He QY. clusterProfiler: an R package for comparing biological themes among gene clusters. OMICS. 2012;16(5):284–7.
21. Shannon P, Markiel A, Ozier O, Baliga NS, Wang JT, Ramage D, et al. Cytoscape: a software environment for integrated models of biomolecular interaction networks. Genome Res. 2003;13(11): 2498–504.
22. Hänzelmann S, Castelo R, Guinney J. GSVA: gene set variation analysis for microarray and RNA-seq data. BMC Bioinformatics. 2013;14:7.
23. Woo HH, Chambers SK. Human ALKBH3-induced m(1)a demethylation increases the CSF-1 mRNA stability in breast and ovarian cancer cells. Biochim Biophys Acta Gene Regul Mech. 2019;1862(1):35–46.
24. Shi Q, Xue C, Yuan X, He Y, Yu Z. Gene signatures and prognostic values of m1A-related regulatory genes in hepatocellular carcinoma. Sci Rep. 2020;10(1):15083.
25. Zheng J, Guo J, Cao B, Zhou Y, Tong J. Identification and validation of lncRNAs involved in m6A regulation for patients with ovarian cancer. Cancer Cell Int. 2021;21(1):363.
26. Li Q, Ren CC, Chen YN, Yang L, Zhang F, Wang BJ, et al. A risk score model incorporating three m6A RNA methylation regulators and a related network of miRNAs-m6A regulators-m6A target genes to predict the prognosis of patients with ovarian cancer. Front Cell Dev Biol. 2021;9:703969.
27. He R, Man C, Huang J, He L, Wang X, Lang Y, et al. Identification of RNA methylation-related lncRNAs signature for predicting hot and cold tumors and prognosis in colon cancer. Front Genet. 2022;13:870945.
28. Francis J, Zvada SP, Denti P, Hatherill M, Charalambous S, Mungofa S, et al. A population pharmacokinetic analysis shows that arylacetamide deacetylase (AADAC) gene polymorphism and HIV infection affect the exposure of rifapentine. Antimicrob Agents Chemother. 2019;63(4):e01964-18.
29. Wang H, Wang D, Gu T, Zhu M, Cheng L, Dai W. AADAC promotes therapeutic activity of cisplatin and imatinib against ovarian cancer cells. Histol Histopathol. 2022;37(9):899–907.
30. Li Y, Yang R, Chen L, Wu S. CD38 as an immunomodulator in cancer. Future Oncol. 2020;16(34):2853–61.
31. Zhu Y, Zhang Z, Jiang Z, Liu Y, Zhou J. CD38 predicts favorable prognosis by enhancing immune infiltration and antitumor immunity in the epithelial ovarian cancer microenvironment. Front Genet. 2020;11:369.
32. Chang X, Dong Y. CACNA1C is a prognostic predictor for patients with ovarian cancer. J Ovarian Res. 2021;14(1):88.
33. Li L, Feng R, Xu Q, Zhang F, Liu T, Cao J, et al. Expression of the β3 subunit of Na(+)/K(+)-ATPase is increased in gastric cancer and regulates gastric cancer cell progression and prognosis via the PI3/AKT pathway. Oncotarget. 2017;8(48):84285–99.
34. Huang W, Zhang Y, Xu Y, Yang S, Li B, Huang L, et al. Comprehensive analysis of the expression of sodium/potassium-ATPase α subunits and prognosis of ovarian serous cystadenocarcinoma. Cancer Cell Int. 2020;20:309.
35. Cramer DW, Welch WR. Determinants of ovarian cancer risk. II. Inferences regarding pathogenesis. J Natl Cancer Inst. 1983; 71(4):717–21.
36. So WK, Cheng JC, Poon SL, Leung PC. Gonadotropin-releasing hormone and ovarian cancer: a functional and mechanistic overview. FEBS J. 2008;275(22):5496–511.
37. Jiang R, Zhang H, Zhou J, Wang J, Xu Y, Zhang H, et al. Inhibition of long non-coding RNA XIST upregulates microRNA-149-3p to repress ovarian cancer cell progression. Cell Death Dis. 2021;12(2):145.
38. Yuan J, Yi K, Yang L. LncRNA NEAT1 promotes proliferation of ovarian cancer cells and angiogenesis of co-incubated human umbilical vein endothelial cells by regulating FGF9 through sponging miR-365: an experimental study. Medicine (Baltimore). 2021;100(3):e23423.

SUPPORTING INFORMATION

Additional supporting information can be found online in the Supporting Information section at the end of this article.

How to cite this article: Zhao J, Han H, Wang R, Wang Y, Zhang Y, Li N, et al. Identification of N1 methyladenosine-related biomarker predicting overall survival outcomes and experimental verification in ovarian cancer. J Obstet Gynaecol Res. 2023. https://doi.org/10.1111/jog.15745